Supporting Information

Electrochemical Conversion of Bulk Platinum into Platinum Single-atom Sites for Hydrogen Evolution Reaction

Zhiyuan Wang,†[a,b] Jia Yang,†[a] Jie Gan,†[c] Wenxing Chen,[d] Fangyao Zhou,[a] Xiao Zhou,[a] Zhenqiang Yu,*[b] Junfa Zhu,[e] Xuezhi Duan,*[c] Yuen Wu*[a]

a. Hefei National Laboratory for Physical Sciences at the Microscale, Collaborative Innovation Center of Chemistry for Energy Materials (iChEM), School of Chemistry and Materials Science, National Synchrotron Radiation Laboratory, University of Science and Technology of China, Hefei, Anhui 230026, China
E-mail: yuenwu@ustc.edu.cn
b. School of Chemistry and Environmental Engineering, Institute of Low-dimensional Materials Genome Initiative, Shenzhen University, Shenzhen 518060, China
E-mail: zqyu@szu.edu.cn
c. State Key Laboratory of Chemical Engineering, East China University of Science and Technology, Shanghai 200237, China
d. Beijing Key Laboratory of Construction Tailorable Advanced Functional Materials and Green Applications, School of Materials Science and Engineering, Beijing Institute of Technology, Beijing 100081, P. R. China
e. National Synchrotron Radiation Laboratory (NSRL), University of Science and Technology of China, Hefei 230026, China

Experimental Section

Materials: Carbon paper (Toray, TGP-H-60) and graphite powder were purchased from Alfa Aesar; analytical grade $Zn(NO_3)_2 \cdot 6H_2O$, 2-methyl imidazole, urea, dicyandiamide, dopamine hydrochloride, methanol, lactic acid, HNO_3, and H_2SO_4 were purchased from Shanghai Chemical Reagents, China. Deionized (DI) water from Milli-Q System (Millipore, Billerica, MA) was used in all our experiments.

Synthesis of ZIF-8: In a typical procedure, $Zn(NO_3)_2 \cdot 6H_2O$ (0.558 g) was dissolved in 15 ml methanol to form homogeneous solution and then continuously injected into 15 ml methanol solution containing 2-methylimidazole (MeIM) (0.616 g). The mixture solution was ultrasound for 10 min at room temperature and then stirred for 12h at 35 ℃. The as-obtained precipitates were collected by centrifugation and washed with methanol for three times and then dried in vacuum at 65 ℃ overnight for further use.

Synthesis of pyrolyzed ZIF-8 (N-C): In a typical procedure, the synthesized ZIF-8 was grinded to powders and then placed in the porcelain boat. Followed this the boat was heated in the tube furnace at 1223 K under argon atmosphere for 2h with a heating rate of 5 K/min. After cooling down to the room temperature, the black powder was stored in a glass bottle for further use.

Synthesis of GO: The graphene oxide (GO) was prepared by a modified Hummer's method. In a typical procedure, 5.0 g graphite powder was added into 180 mL concentrated H_2SO_4, the mixture was stirred for 1h. Then 60 mL concentrated HNO_3 was slowly added into the mixture under ice-bath and continuously stirring. After the temperature cooling down, 25 g $KMnO_4$ was slowly added under ice-bath and stirring. Then the obtained slurry was stirred at room temperature for 120 h. Subsequently, 600 mL deionized (DI) water was slowly added into the slurry and the mixture was stirred for another 2 h. Then 30 mL 30% H_2O_2 was added, the solution color immediately turned into a bright yellow. The solution was stirred for 2 h and then stand for 10 h, the supernatant was poured and the rest mixture was transferred into a

dialysis bag (MD31), which was seeking into the DI-water until the pH was at about 7.0. Then the mixture was stored in a glass bottle for further use.

Synthesis of GOM: The obtained GO solution was filtered under vacuum with a microporous membrane (Φ50 mm, 0.22 μm) for 10h until an obvious yellow layer formed. Then the graphene oxide membrane can be obtained after the microporous membrane was dried at room-temperature.

Synthesis of Pt-SAs/C: The Pt-SAs/C was prepared via an electro-filtration method in a three-electrode H-cell, in which 30.0 mL 0.5mol/L H_2SO_4 solution was used as electrolyte, Pt foil, Ag/AgCl (saturated KCl) and the commercial carbon paper were used as counter electrode, reference electrode and working electrode, respectively. And the graphene oxide membrane (GOM) was used as the separator between the CE and WE. Before electrochemical deposition, the carbon paper was treated with ethanol, acetone and DI-water, respectively. The electrodeposition was conducted at 5 mA cm^{-2} for different time (1-12h) at room temperature, and the solution in both sides of H-cell are continuously stirring slightly with magnetic stirring bar. After a thorough washing with DI-water, the deposited WE was dried at 80℃ overnight under vacuum.

Synthesis of Pt-NP/C: The Pt-NP/C was prepared via the same procedure as the Pt-SAs/C except without using GOM as the separator. In the three-electrode H-cell, the Pt foil, Ag/AgCl (saturated KCl) and the commercial carbon paper were used as counter electrode, reference electrode and working electrode, respectively; and 20.0 mL 0.5mol/L H_2SO_4 solution was used as electrolyte. The electrochemical deposition was conducted at 5 mA cm^{-2} for different time (1-12h) at room temperature. After a thorough washing with DI-water, the deposited WE was dried at 80℃ overnight under vacuum.

Synthesis of Au-SAs/C and Ru-SAs/C: The Au-SAs/C and Ru-SAs/C were prepared by the same method as the Pt-SAs/C. In the three-electrode H-cell, the Au wire/Ru wire, Ag/AgCl (saturated KCl) and the commercial carbon paper were used as counter electrode, reference

electrode and working electrode, respectively; and 20.0 mL 0.5mol/L H_2SO_4 solution was used as electrolyte. The electrochemical deposition was conducted at 5 mA cm^{-2} for different time (1-12h) at room temperature. After a thorough washing with DI-water, the deposited WE was dried at 80℃ overnight under vacuum.

Synthesis of Pt-SAs/N-C: The Pt-SAs/N-C was prepared via an electro-filtration method in a three-electrode H-cell, in which 20.0 mL 0.5mol/L H_2SO_4 solution was used as electrolyte, Pt foil and Ag/AgCl (saturated KCl) were used as counter electrode and reference electrode, respectively. And the graphene oxide membrane (GOM) was used as the separator between the CE and WE. Firstly, the working electrode was prepared by dropping the pyrolyzed ZIF-8 (N-C) ethanol solution at graphite paper, after drying there was a thin layer of N-C coated on the graphite paper. Electrodeposition was conducted at 5mA cm^{-2} for different time at room temperature. After a thorough washing with DI-water, the WE was sonicated for 2h in a beaker containing 5ml DI-water, and the Pt-SAs/N-C was collected by centrifugation and dried at 80℃ overnight under vacuum.

Synthesis of ultrathin nitrogen doped carbon nanosheet (U-N/C): In a typical synthesis, 0.8408g (10 mmol) dicyandiamide and 0.0948g (0.5 mmol) dopamine hydrochloride were grinded in agate mortar for 20 min, after well mixed, the mixture was transferred into a crucible, and heated in the tube furnace at 1073 K under argon atmosphere for 2h with a heating rate of 5 K/min. After cooling down to the room temperature, the black powder was grinded and stored in a glass bottle for further use.

Synthesis of Pt-SAs/U-N/C and Au-SAs/U-N/C: The Pt-SAs/U-N/C and Au-SAs/U-N/C were prepared by the same method as the Pt-SAs/N-C.

Synthesis of CdS nanorod: CdS nanorod was prepared by the previous method. In a typical synthesis, 5.4 mmol of $Cd(NO_3)_2 \cdot 4H_2O$ were dissolved in 108 mL ethylenediamine and stirred at room temperature for 30 min to obtain a uniform solution. After that, 10.8 mmol of thiourea were added to the solution, which was stirred for another 30 min. Then the mixture

was transferred into a 100 mL Teflon-lined stainless-steel autoclave and maintained at 180 °C for 12 h. The final products were washed with deionized water and ethanol for several times to remove any possible ions and then dried at 60 °C under vacuum for a couple of hours.

Synthesis of Pt-SAs/C@CdS: The synthesized Pt-SAs/C was firstly grinded into fine powder, then 2 mg grinded powder was dispersed into 50 mL ethanol at room temperature under sonication. Subsequently, 100 mg CdS NR was added to the dispersed solution. Then the mixture was sonicated for 2h, the precipitate was separated by centrifugation and washed several times with water and ethanol, and then dried at 60 °C under vacuum overnight.

Characterization: Powder X-ray diffraction patterns of samples were recorded on a Rigaku Miniflex-600 operating at 40 KV voltage and 15 mA current with Cu Kα radiation (λ=0.15406 nm). TEM was recorded on a Hitachi-7700 working at 100 kV. HAADF-STEM images and the EDS of samples were performed with a JEOL JEM-2010 LaB6 high-resolution transmission electron microscope operated at 200 kV. The SEM was performed on JSM-6700F. The ICP measurement was performed on Optima 7300 DV. X-ray photoelectron spectroscopy (XPS) was collected on scanning X-ray microprobe (PHI 5000 Verasa, ULAC-PHI, Inc.) using Al Ka radiation and the C1s peak at 284.8 eV as internal standard. Raman scattering spectra were recorded with a Renishaw System 2000 spectrometer using the 514.5 nm line of Ar+ for excitation.

XAFS measurement and data analysis: XAFS spectra at the Pt L_3-edge were collected at the beamline 14W1 at the Shanghai Synchrotron Radiation Facility (SSRF), Shanghai Institute of Applied Physics, China, and operated at 3.5GeV third generation synchrotron source with injection currents of 140–210 mA in transmission mode, using a Si (111) double-crystal monochromator to reduce the harmonic component of the monochrome beam. Pt foil and PtO_2 were used as reference samples and measured in the transmission mode. All samples were pelletized as disks of 13 mm diameter using graphite powder as a binder. The acquired EXAFS data were processed according to the standard procedures using the ATHENA

module implemented in the IFEFFIT software packages. The EXAFS spectra were obtained by subtracting the post-edge background from the overall absorption and then normalizing with respect to the edge-jump step. The NEXAFS spectra (C K-edge) were measured at Hefei NSRL station. Synchrotron-radiation photoemission spectroscopy experiments were performed at the Photoemission Endstation (BL10B) at Hefei NSRL station.

The valence-band spectra were measured using synchrotron-radiation light as the excitation source with a photon energy of 40.0 eV and referenced to the Fermi level ($E_F = 0$) determined from Au. The work function (Φ) was determined by the difference between the photon energy and the width of whole valence-band spectra. A sample bias of −10 V was applied for the secondary electron cutoff. UV-vis-NIR diffuse reflectance spectra were recorded in the spectral region of 240-1200 nm with a Shimadzu SolidSpec-3700 spectrophotometer. Ultraviolet-visible diffuse reflectance spectra were collected for the dry-pressed disk samples with an ultraviolet-visible spectrophotometer (UV2600, Shimadzu, Japan) using $BaSO_4$ as the reflectance standard. Steady-state photoluminescence (PL) spectra were recorded on a JY Fluorolog-3-Tou Spectrometer and a FluoroMax-4 spectrofluorometer (Horiba Scientific). Time-resolved PL decay spectra were collected on an FLS920 fluorescence lifetime spectrophotometer (Edinburgh Instruments, UK) under the excitation of 365 nm and probed at 460 nm. The amounts of H_2 evolved were determined using gas chromatograph (Techcomp GC-7900, China) equipped with a TDX-01 packed column. H_2 was detected using a thermal conductivity detector.

Electrochemical measurements: Electrochemical measurements were performed with a CHI 760E electrochemical workstation in a standard three-electrode system in 0.5 M H_2SO_4 solution at room temperature, using the synthesized Pt-SAs carbon paper electrode as the working electrode (1×1 cm^2 in area), a graphite rod as the counter electrode, and a Ag/AgCl electrode (saturated KCl) as the reference electrode. For commercial 20% Pt/C, the working

electrode was prepared by dropping 200 uL well-dispersed catalysts ink on a carbon paper (1×1 cm^2 in area) and dried at 60 °C for 2h. The catalyst ink was prepared by dispersing 5 mg 20% Pt/C and 20 uL 5wt% Nafion in 1 mL ethanol/water (1/1, v/v) solution and sonicated for 30 min. In all measurements, the Ag/AgCl reference electrode was calibrated with respect to the reversible hydrogen electrode (RHE). In H_2 saturated 0.5M H_2SO_4, E (RHE) = E (Ag/AgCl) + 0.197 V + 0.059 × pH. The HER was performed in Ar-saturated 0.5 M H_2SO_4 solution with a scan rate of 5 mV s^{-1}.

Photocatalytic activity measurements: Photocatalytic hydrogen reactions were carried out in a 50 mL quartz reactor at 25 °C and atmospheric pressure. Typically, the prepared Pt-SAs-C@CdS (10 mg) was dispersed into 10 mL containing 10% lactic acid aqueous solution and sonicated for 30 minutes. A 300 W Xe lamp equipped with a UV light filter ($\lambda > 420$ nm) was employed as a visible light source. Prior to visible light irradiation the solution was thoroughly degassed with Ar gas for 2 h to remove dissolved oxygen. The evolved H_2 was analyzed by a gas chromatograph (Techcomp GC-7900, China) with a thermal conductivity detector. Ultrapure nitrogen was used as a carrier gas.

Photoelectrochemical measurements: Photocurrent was measured in the three-electrode system with utilizing the synthesized samples as the working electrodes, Pt mesh as the counter electrode, and Ag/AgCl (saturated KCl) as a reference electrode. A 300 W Xe light with a cutoff filter (>420 nm) was used as the light source. 0.5 M Na_2SO_4 mixed aqueous solution was used as the electrolyte. The working electrodes were synthesized as follows: 10 mg sample was dispersed in 1 mL containing 20 uL 5wt% Nafion ethanol/water (1/1, v/v) solution and sonicated for 30 min to make a slurry. Then the slurry was coated onto a fluorine-doped tin oxide (FTO) glass electrode with area of 1.0 cm × 1.0 cm. The obtained electrode was dried at 60 °C for 2 h under flowing N_2. EIS measurements were performed on a CHI 760E electrochemical workstation in a standard three-electrode system utilizing the synthesized samples as the working electrodes, Ag/AgCl (saturated KCl) as a reference

electrode, Pt mesh as the counter electrode, and 0.5 M Na_2SO_4 aqueous solution as the electrolyte. The EIS were recorded over a range from 100 mHZ to 100 KHz with an AC amplitude of 0.02 V.

Computational details: All DFT calculations were performed using the Vienna ab initio simulation package (VASP). The projector augmented wave (PAW) method was employed to describe the interactions between ion cores and valence electrons. The GGA-PBE was used to describe the exchange-correlation functional. The solution of the Kohn-Sham equations was expanded in a plane wave basis set with a cutoff energy of 400 eV. The Brillouin zone sampling was performed using a Monkhorst-Pack grid, and electronic occupancies were determined in light of a Gaussian smearing with a width of 0.05 eV. In all the calculations, a force-based conjugated gradient method was used to optimize the geometries. Saddle points and minima were considered to be converged when the maximum force in each degree of freedom was less than 0.03 eV $Å^{-1}$. Bader charge analysis was implemented with a fast algorithm developed by Henkelman and coworkers, and the core charges were included in the partitions. The charge density difference images were obtained by VESTA visualization software and calculated as $\Delta\rho(r) = \rho_{Pt1\text{-}C4}(r) - \rho_{Pt\text{-}SAs}(r) - \rho_{support}$ and $\Delta\rho(r) = \rho_{defect\text{-}C}(r) - \rho_{H}(r) - \rho_{support}$, where the $\rho(r)$ is the electron density.

All of the graphene models are constructed based on the graphene basal plane model with the supercell of $5 \times 3\sqrt{3} \times 1$ (12.30 Å × 12.78 Å × 15.00 Å). The Brillouin-zone integration has been performed with a 3 × 3 × 1 Monkhorst-Pack k-point mesh. The Pt(111) was modelled using a p(2 × 2) supercell slab model based on bulk fcc Pt crystal whose lattice constant was 3.98 Å, containing four atomic layers slabs, with a relaxation of the top two layers. The Brillouin-zone integration has been performed with a 5×5×1. A vacuum thickness of 12 Å was used to avoid the interaction from the top supercells.

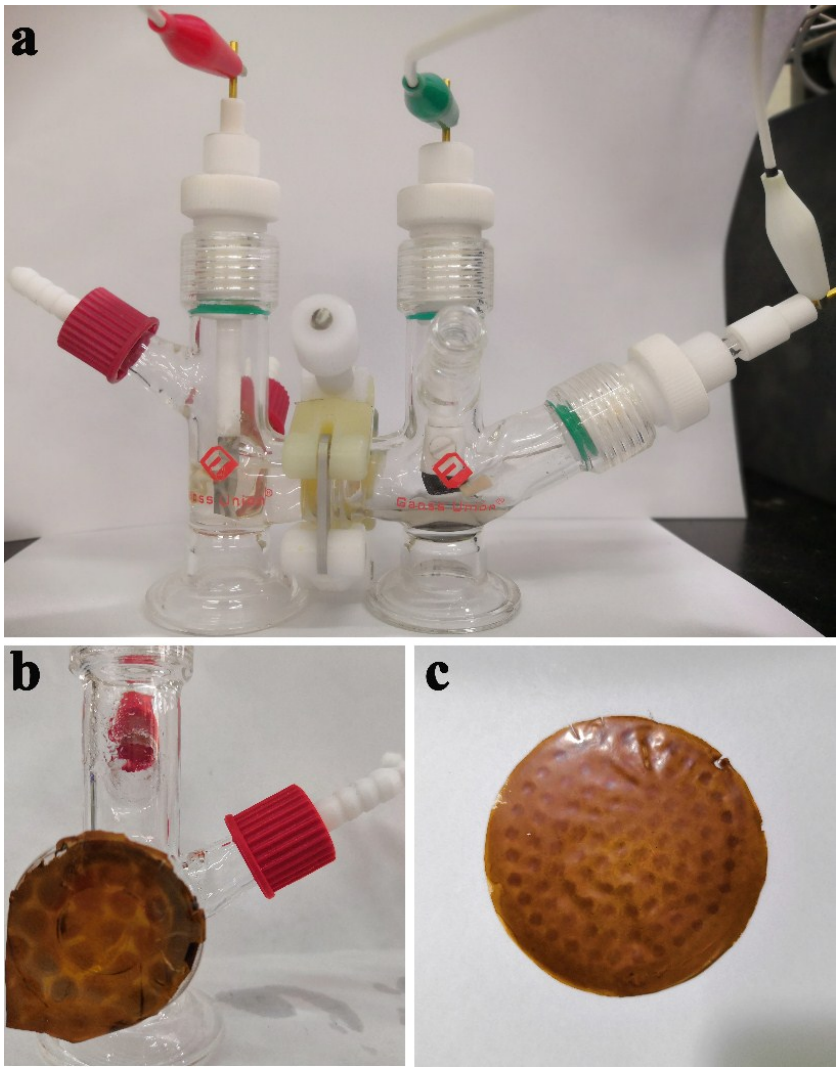

Figure S1. (a) Image of the H-cell for Pt-SAs/C preparation. Images of GOM (b) after and (c) before electrochemical deposition.

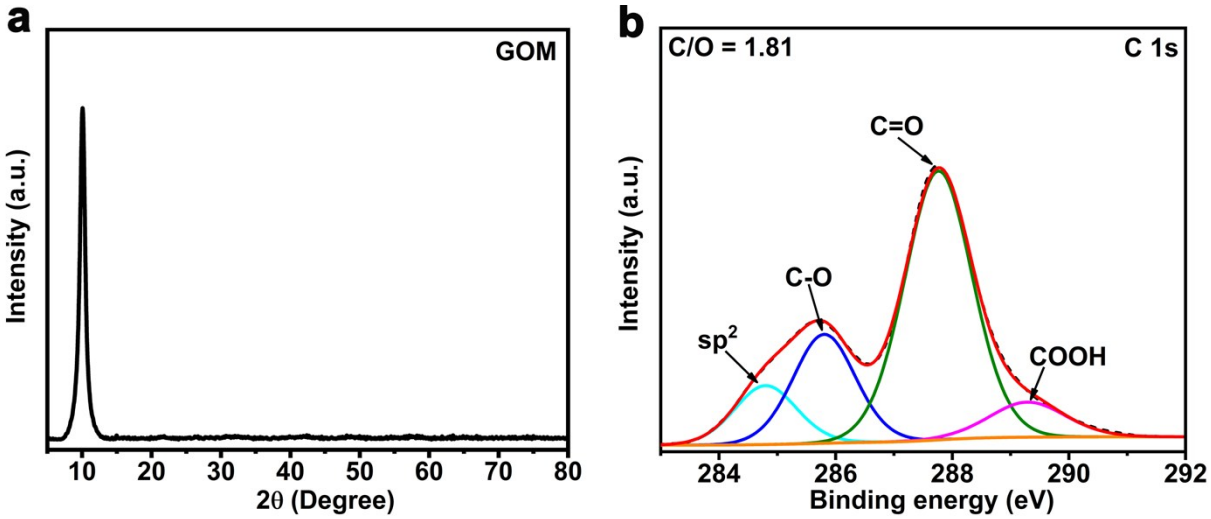

Figure S2. (a) XRD pattern of GOM. (b) The detailed analysis of C 1s spetrum of GOM.

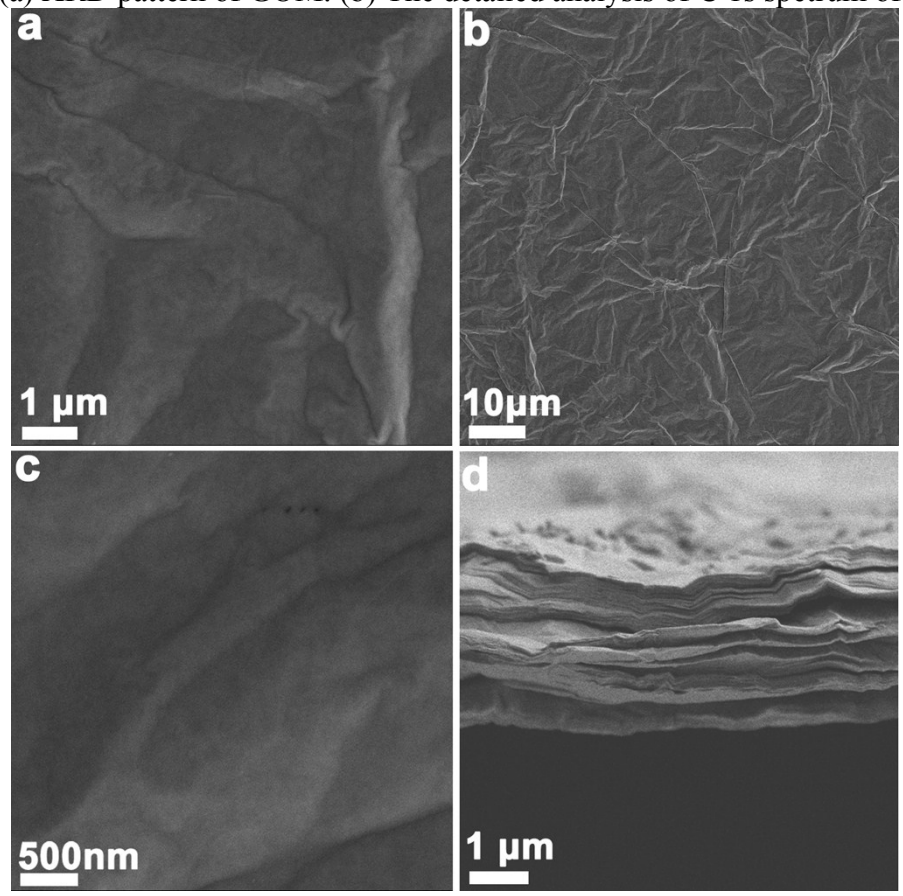

Figure S3. (a) (b) (c) SEM images of GOM with different magnification. (d) SEM images of GOM from side view.

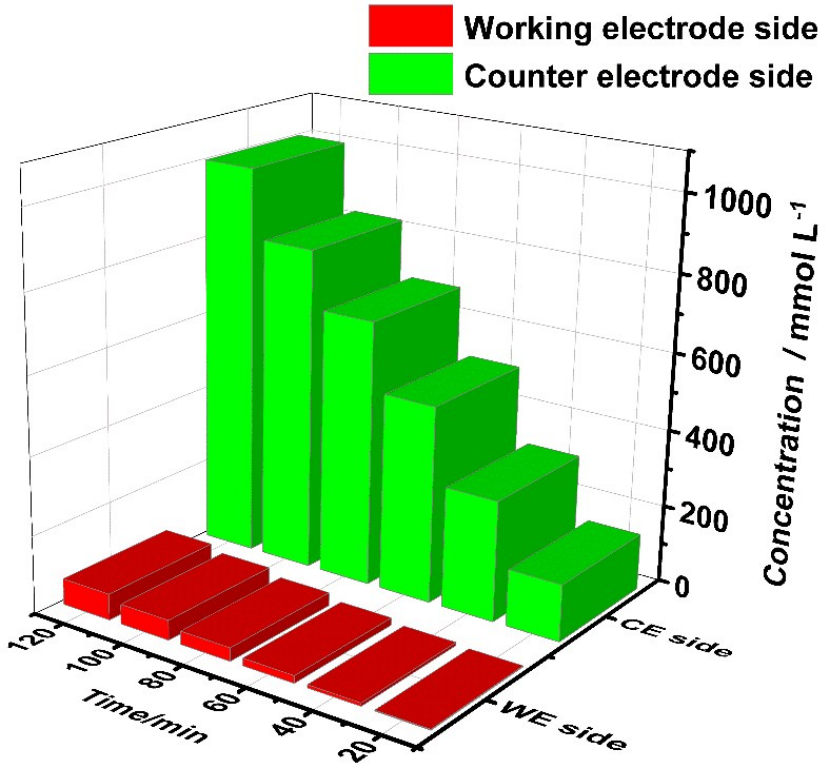

Figure S4. Concentrations of Pt ions on the different sides of GOM during electrochemical deposition.

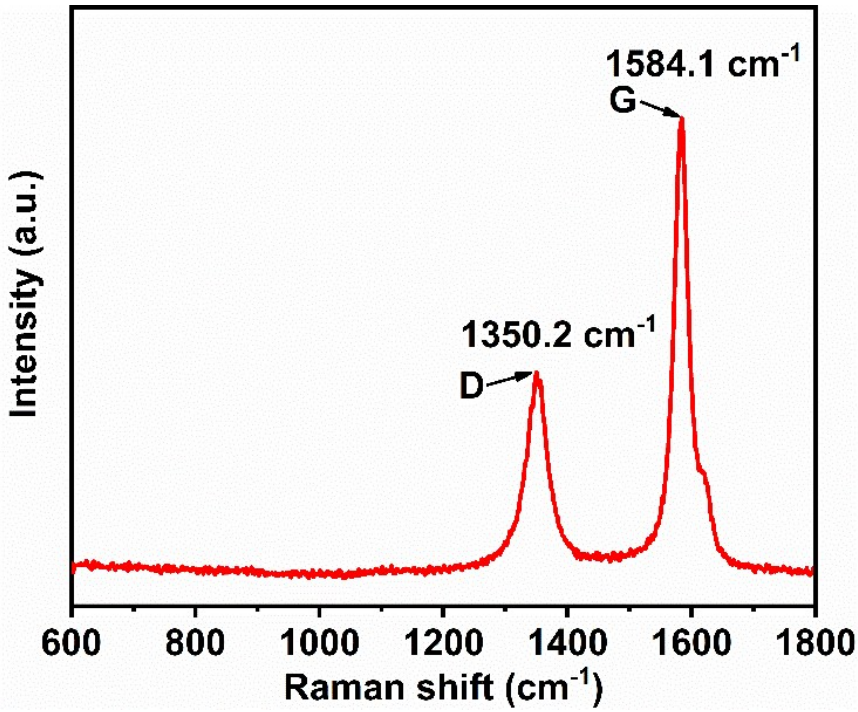

Figure S5. Raman shift of carbon paper.

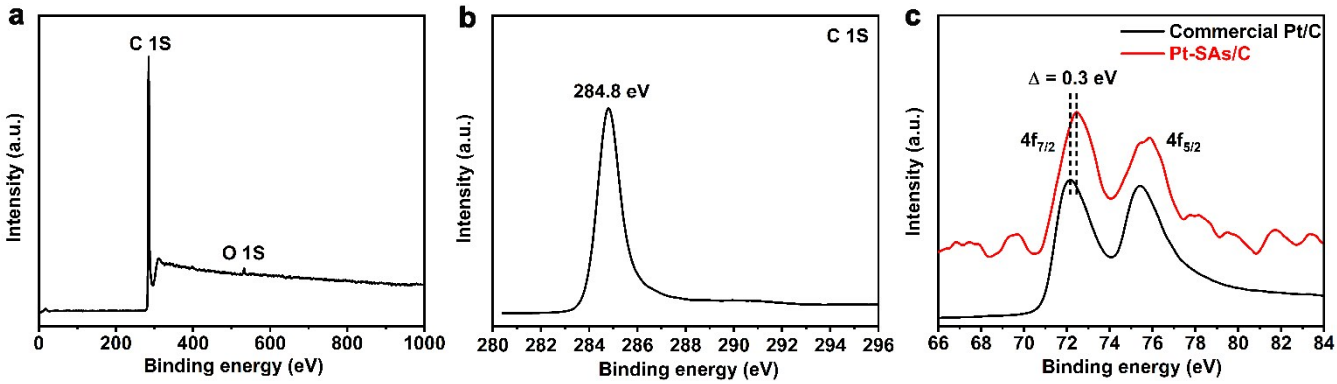

Figure S6. XPS spectra for the (a) survey scan, (b) C 1s, and (d) Pt 4f regions of Pt-SAs/C.

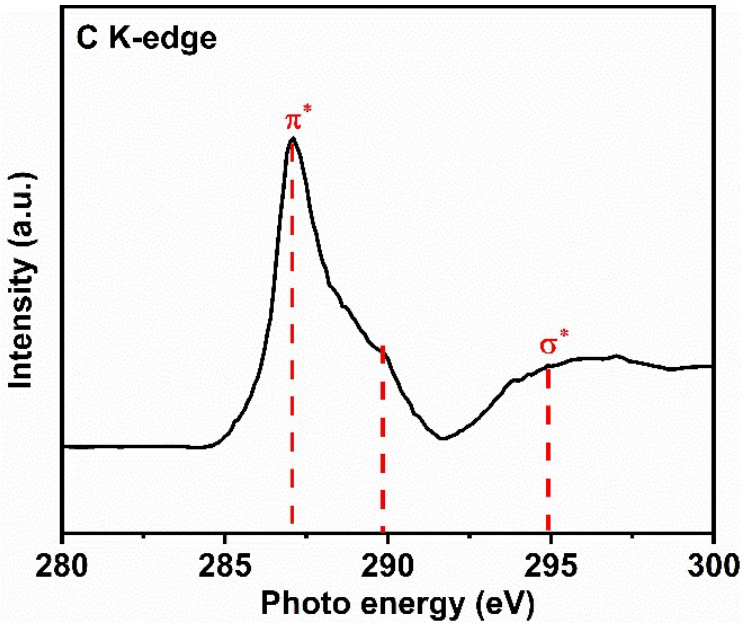

Figure S7. C K-edge NEXAFS spectra of Pt-SAs/C.

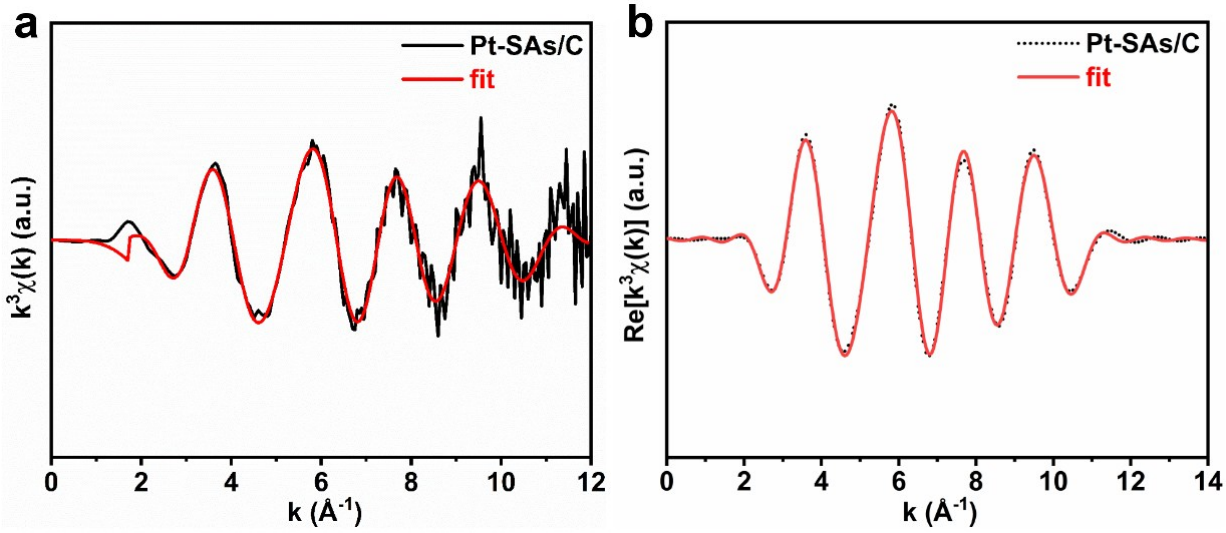

Figure S8. The k^3-weighted EXAFS spectra of Pt-SAs/C and the corresponding fitted curves of $k^3\chi(k)$ oscillation functions in k-space (a) and their Fourier transforms in R space for Pt-SAs/C (b).

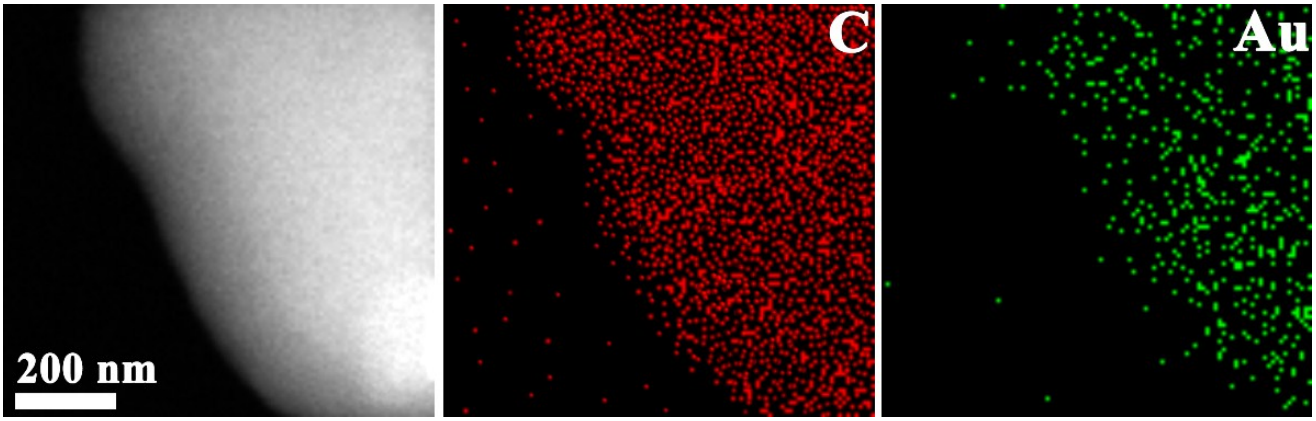

Figure S9. HTEM image and corresponding EDS element maps of Au-SAs/C.

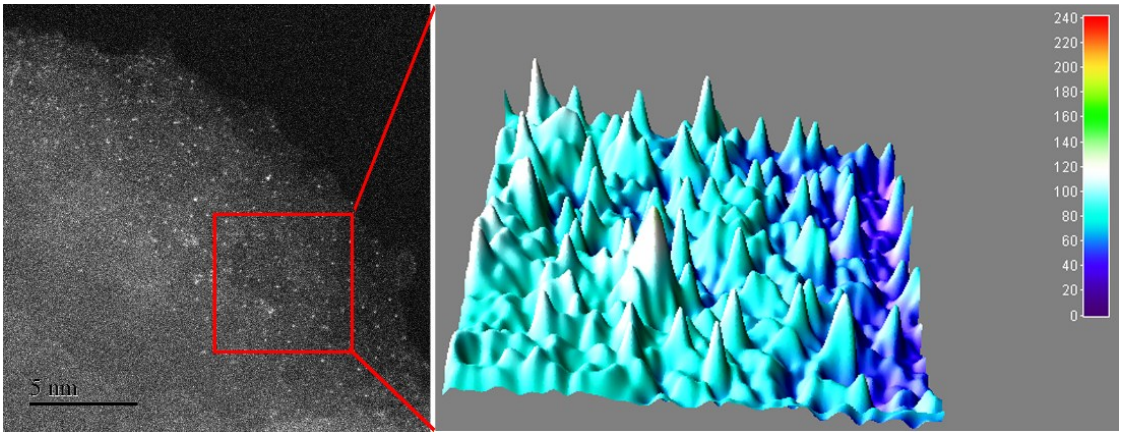

Figure S10. Aberration corrected HAADF-STEM image of Au-SAs/C and the corresponding 3D image for selected area.

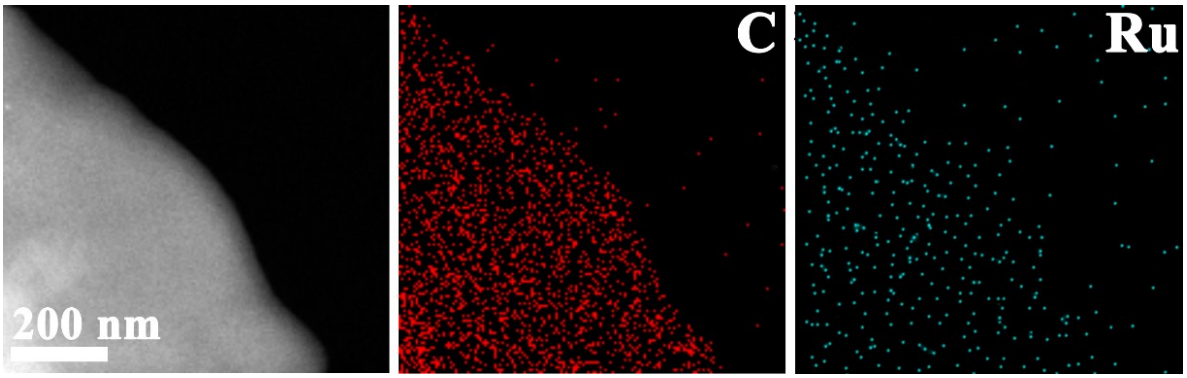

Figure S11. HTEM image and corresponding EDS element maps of Ru-SAs/C.

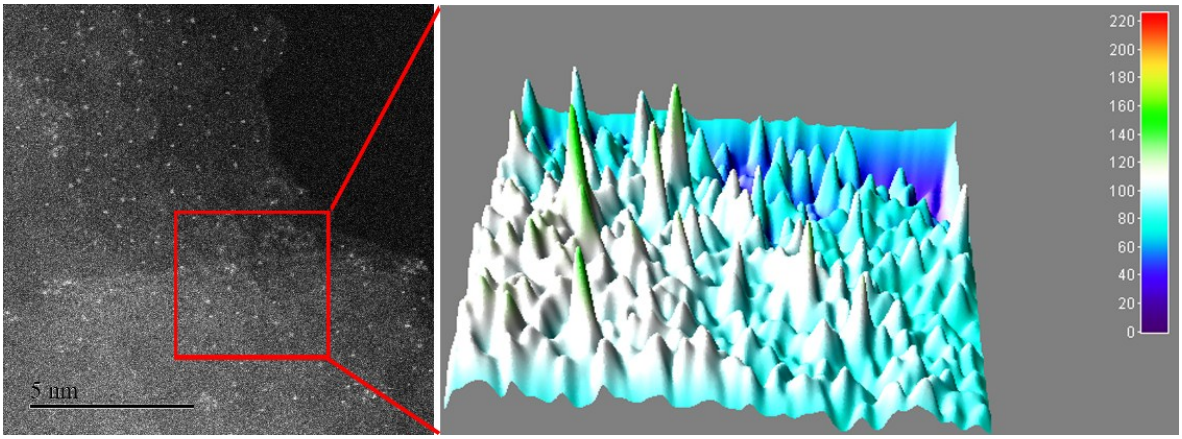

Figure S12. Aberration corrected HAADF-STEM image of Ru-SAs/C and the corresponding 3D image for selected area.

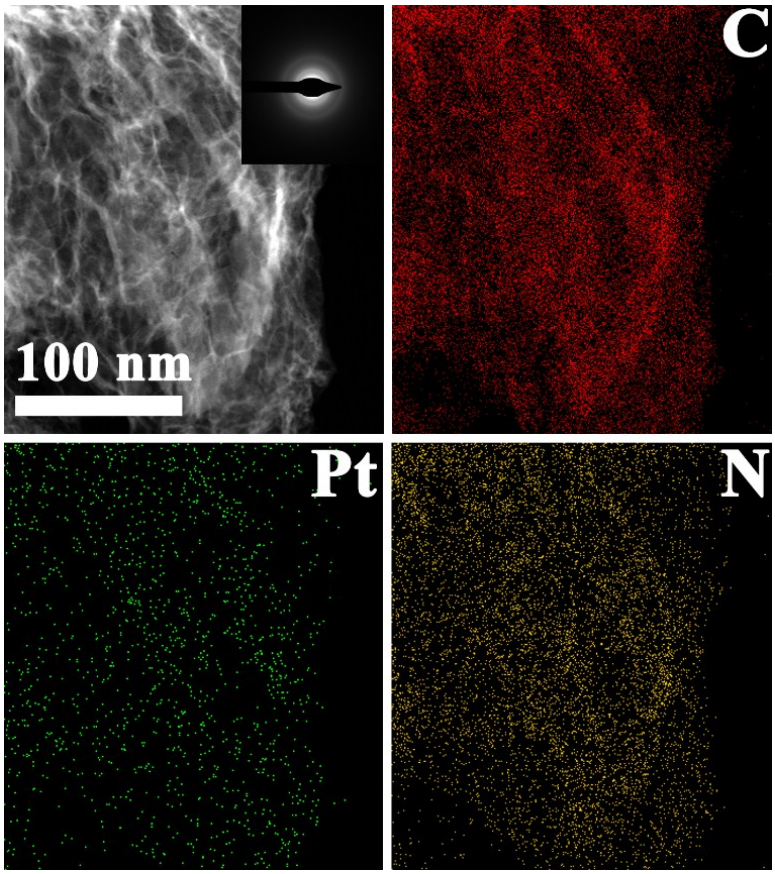

Figure S13. HTEM image and corresponding EDS element maps of Pt-SAs/U-N-C.

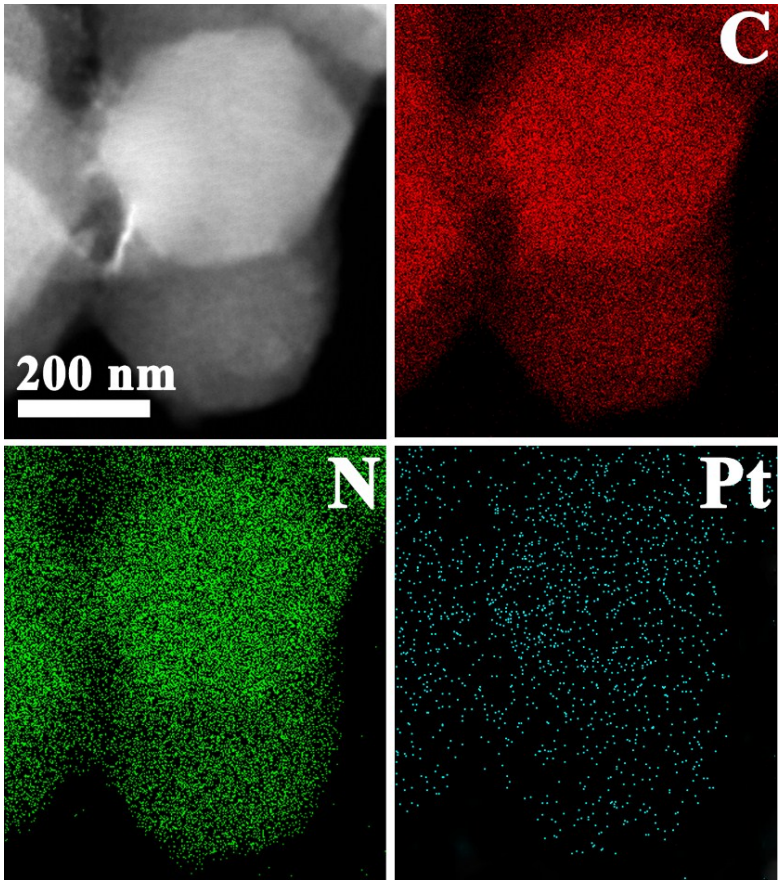

Figure S14. HTEM image and corresponding EDS element maps of Pt-SAs/pyrolyzed ZIF8.

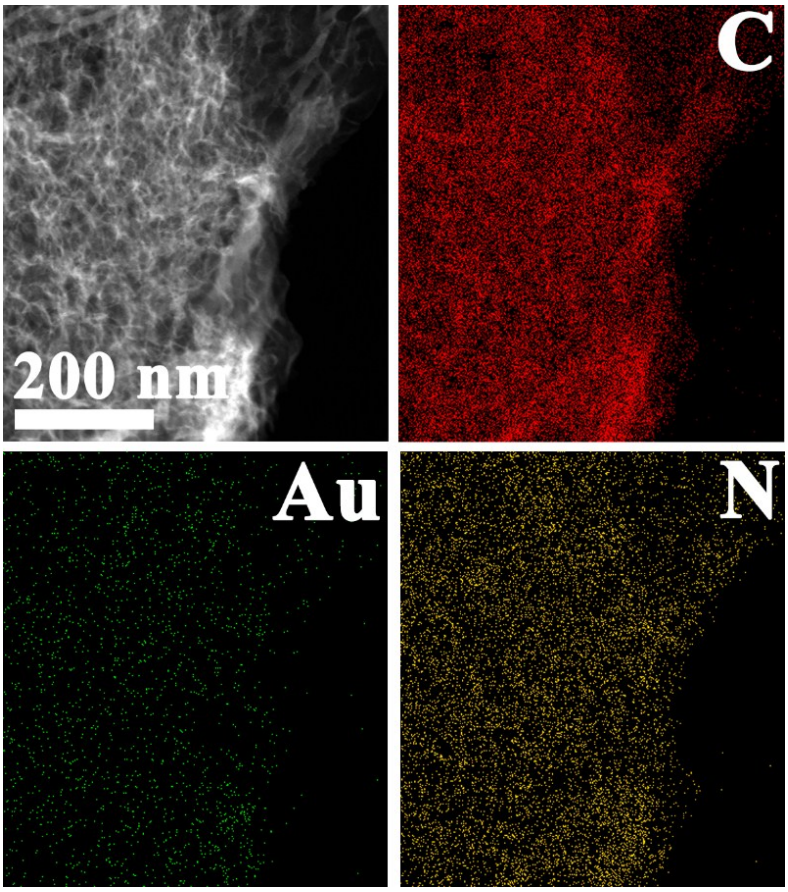

Figure S15. HTEM image and corresponding EDS element maps of Au-SAs/U-N-C.

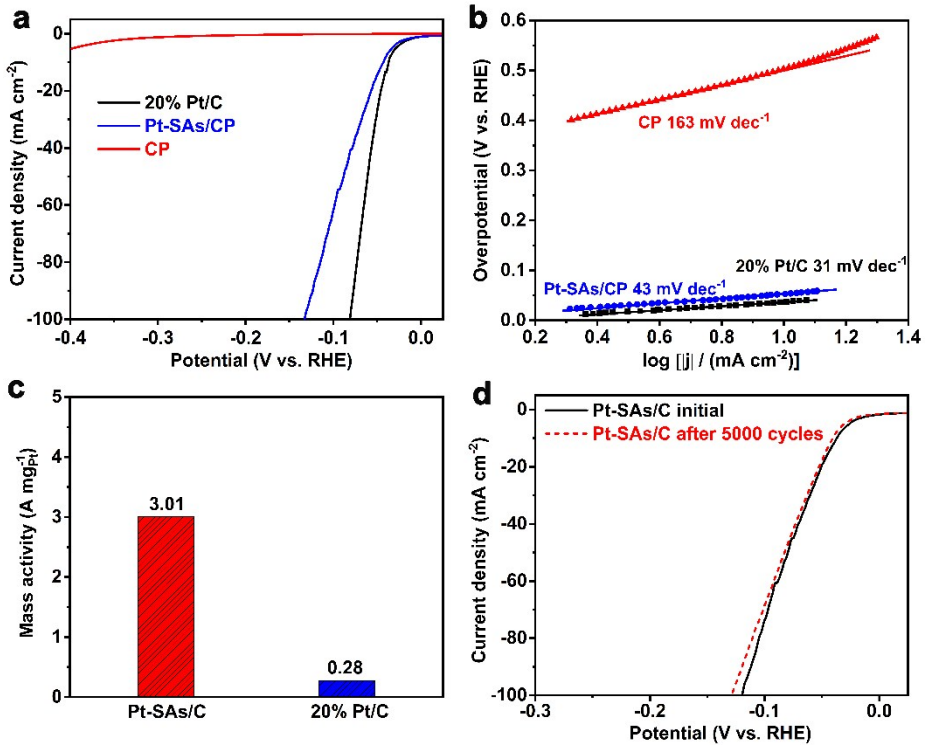

Figure S16. (a) The HER polarization curves and (b) the corresponding Tafel plots of the CP, commercial 20% Pt/C and Pt-SAs/C. (c) The mass activity of commercial 20% Pt/C and Pt-SAs/C at η = 50 mV. (d) Polarization curves recorded in Ar-saturated 0.5 M H_2SO_4 before and after 5000 CV cycles.

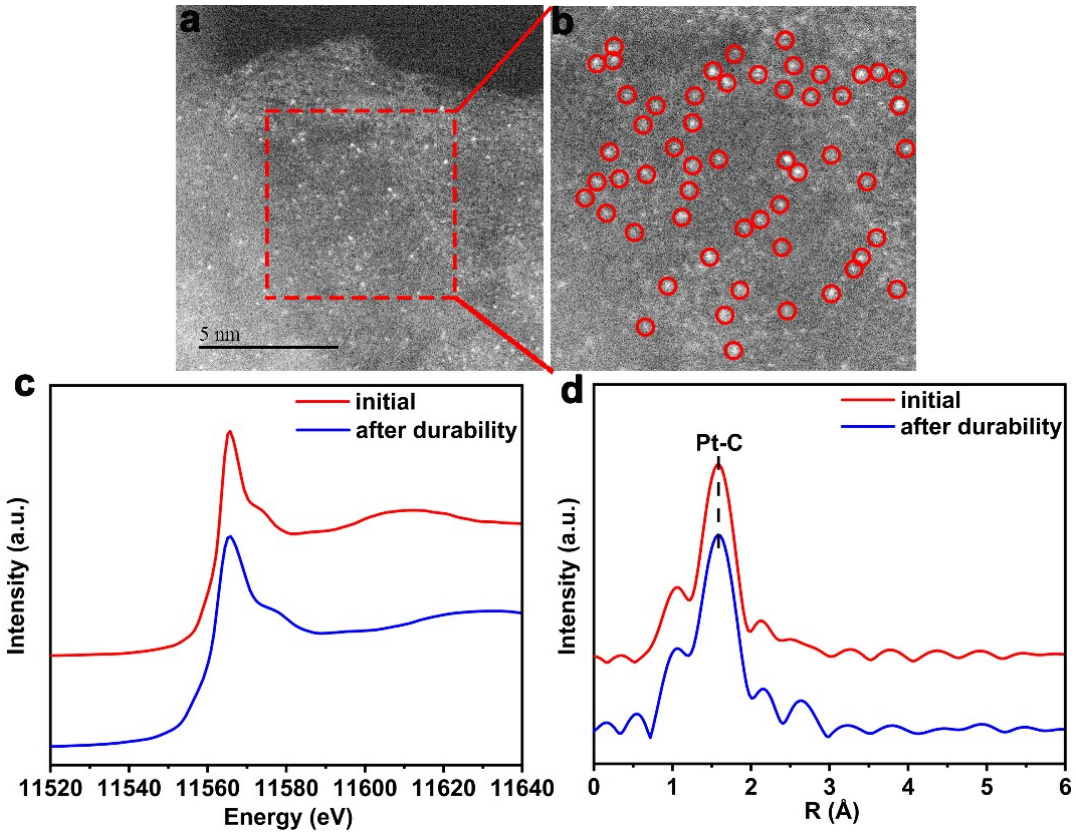

Figure S17. (a) HAADF-STEM and (b) magnified HAADF-STEM images of Pt-SAs/C catalyst after HER durability test. The result reveals the atomically dispersed Pt atoms remained unchanged. c) Pt L_3-edge XANES and (d) k^3-weighted R-space FT spectra from EXAFS of Pt-SAs/C before and after HER durability test.

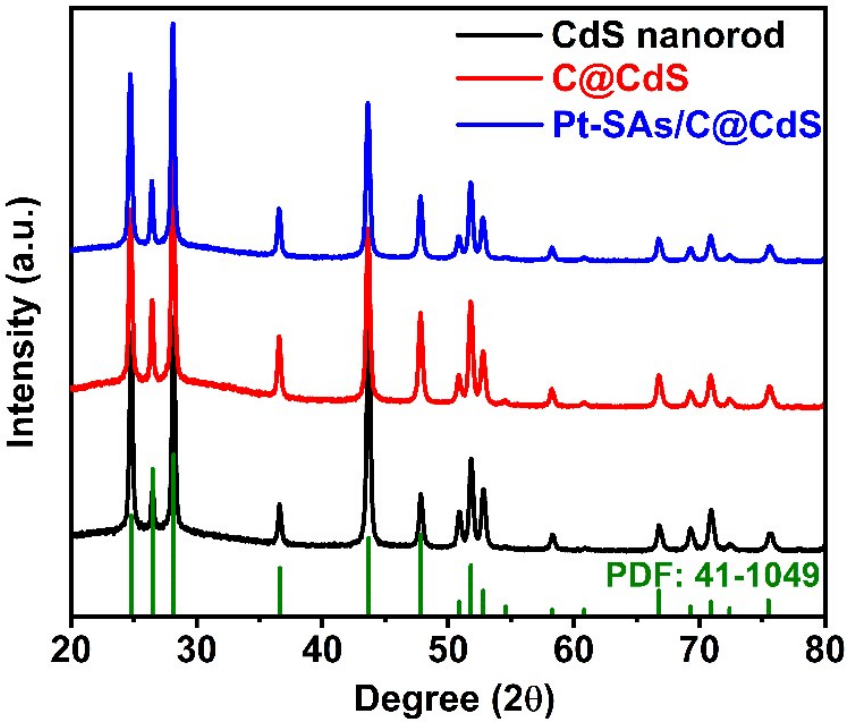

Figure S18. Powder XRD patterns of CdS nanorod, C@CdS and Pt-SAs/C@CdS.

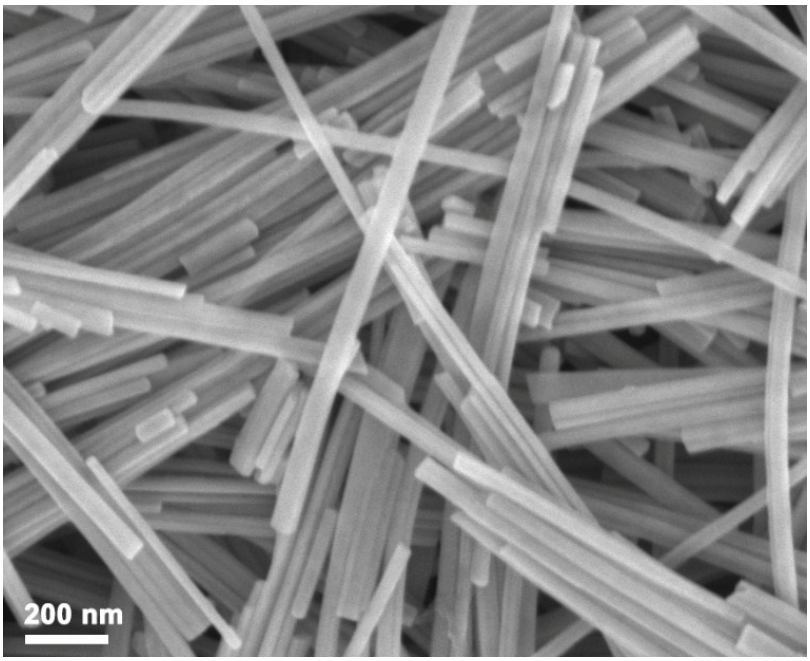

Figure S19. SEM image of Pt-SAs/C@CdS.

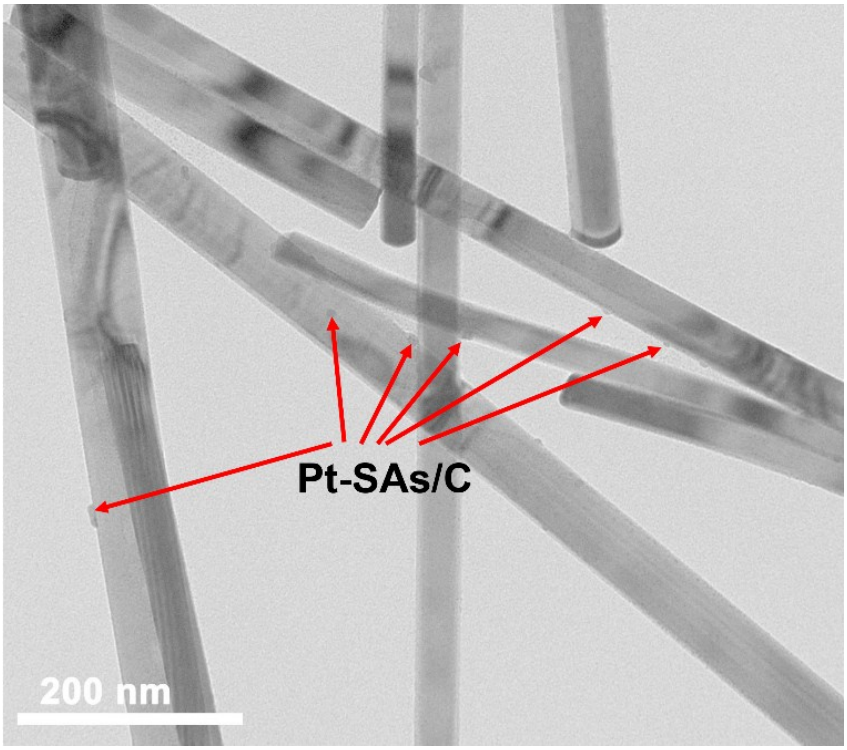

Figure S20. TEM image of Pt-SAs/C@CdS.

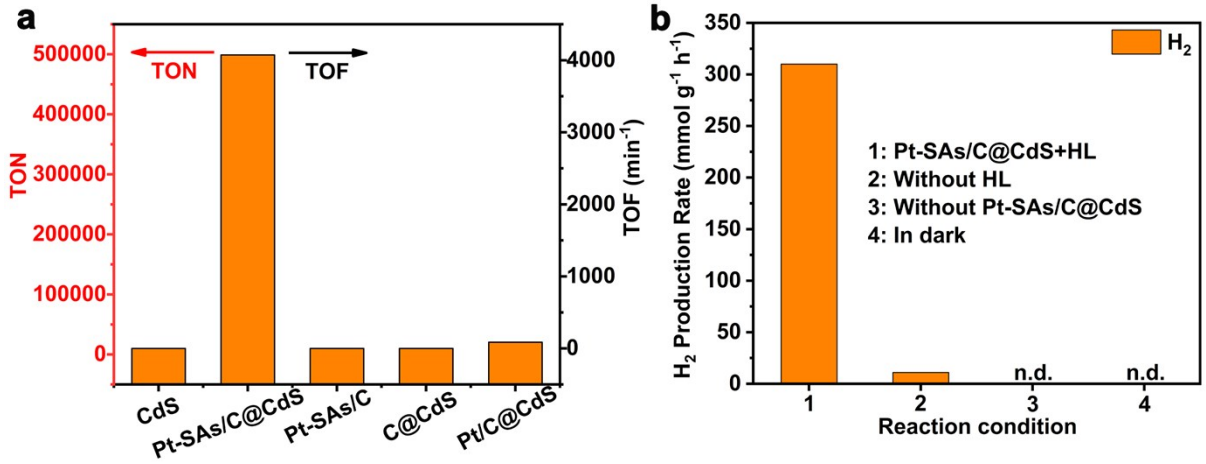

Figure S21. (a) TON and TOF of CdS, Pt-SAs/C@CdS, Pt-SAs/C, Pt/C@CdS and C@CdS under visible light irradiation ($\lambda > 420$ nm). (b) Photocatalytic hydrogen evolution in different conditions. HL is the abbreviation of lactic acid.

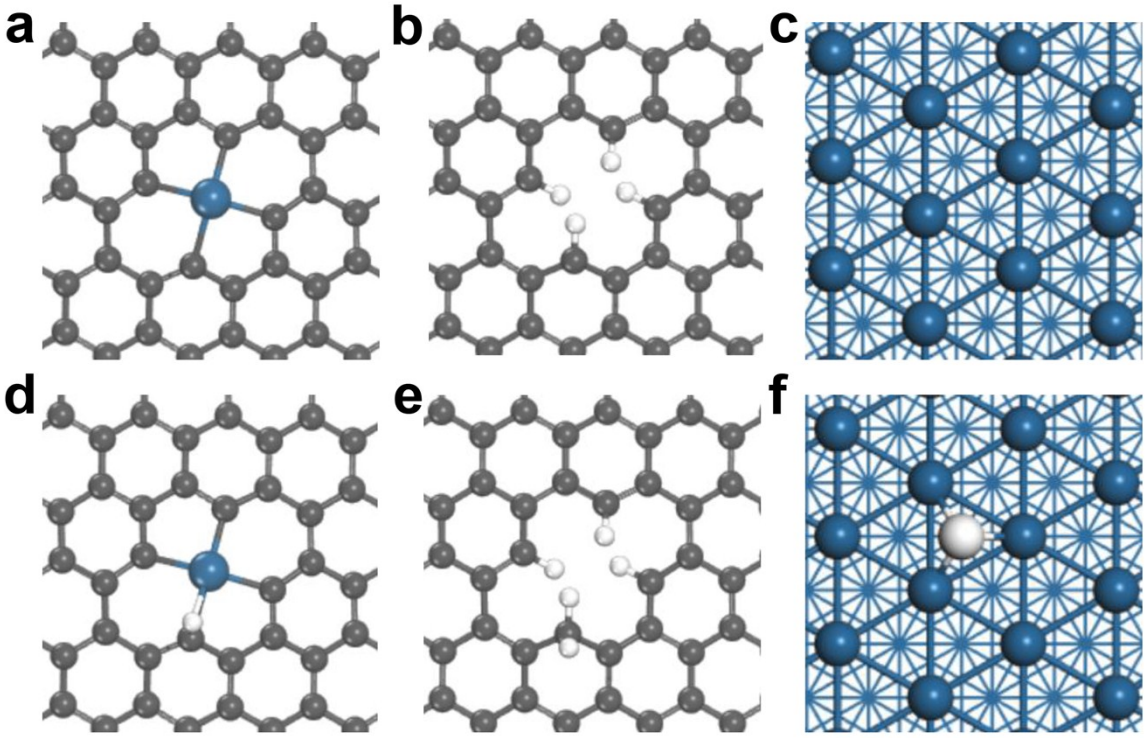

Figure S22. Top view of the optimized structures of (a) Pt-SAs supported on the defect carbon, (b) defect-C, and Pt(111) and their corresponding configuration with adsorbed H (d-f). Blue, gray and write balls represent Pt, C and H atoms, respectively.

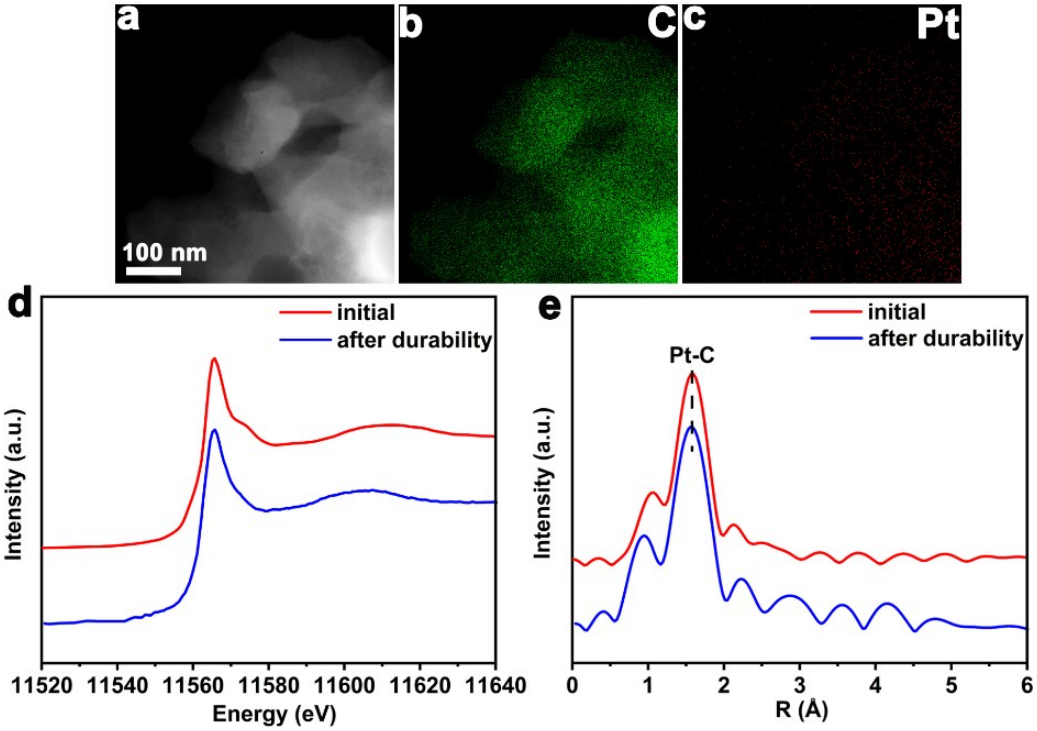

Figure S23. (a) HTEM and (b), (c) corresponding EDS element maps of Pt-SAs/C catalyst after photocatalytic H2 evolution durability test. c) Pt L_3-edge XANES and (d) k^3-weighted R-space FT spectra from EXAFS of Pt-SAs/C before and after photocatalytic H2 evolution durability test.

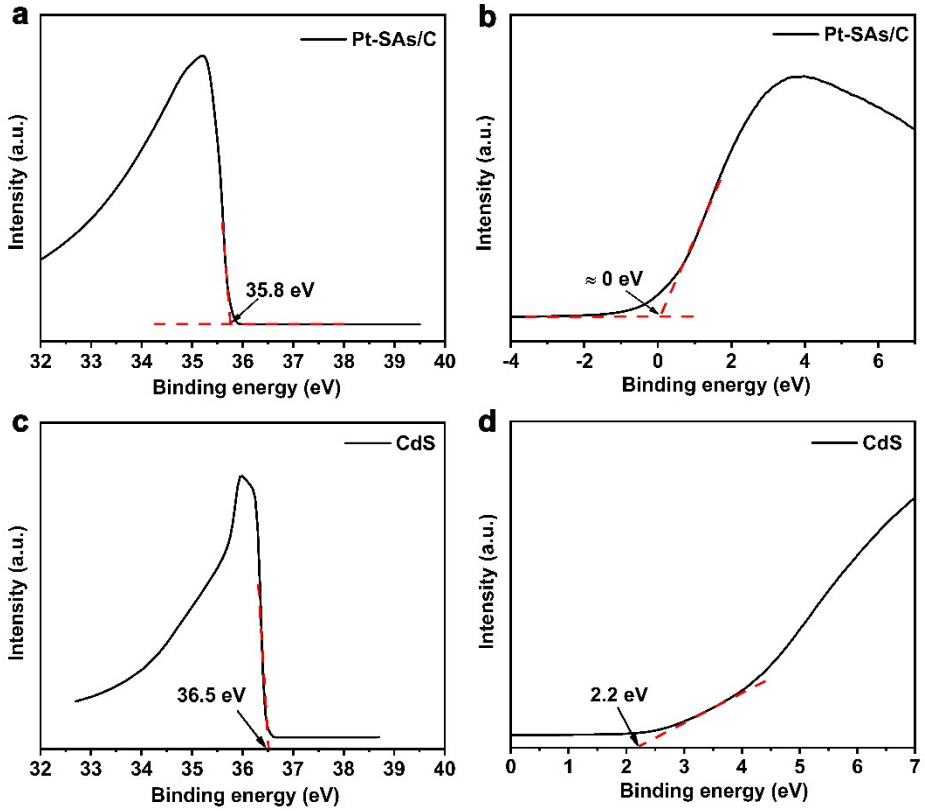

Figure S24. (a) Secondary electron cutoff spectrum and (b) valence-band spectrum of Pt-SAs/C measured by SRPES. (c) Secondary electron cutoff spectrum and (d) valence-band spectrum of CdS measured by SRPES. The excitation photon energy is 40.0 eV.

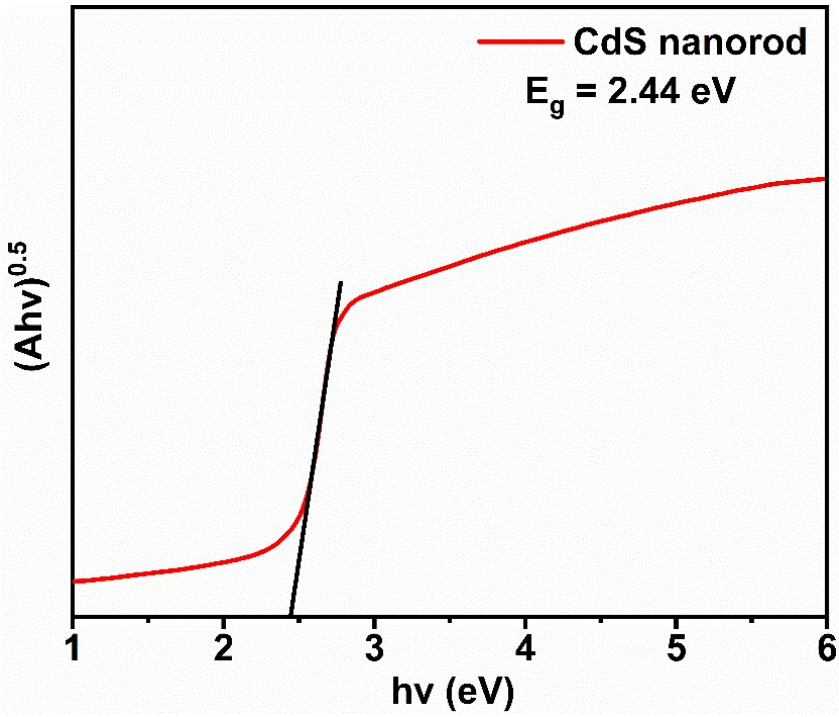

Figure S25. The plot of $(Ahυ)^{0.5}$ versus hυ for calculating the band gap of CdS nanorod from UV-vis-IR diffuse reflectance spectrum of CdS nanorod.

Table S1. Structural parameters extracted from the Pt L_3-edge EXAFS fitting. (S_0^2=0.86)

sample	Scattering pair	CN	R(Å)	$\sigma^2(10^{-3}Å^2)$	ΔE_0(eV)	R factor
Pt-SAs/C	Pt-C	3.9	1.97	6.2	1.5	0.005

S_0^2 is the amplitude reduction factor; CN is the coordination number; R is interatomic distance (the bond length between central atoms and surrounding coordination atoms); σ^2 is Debye-Waller factor (a measure of thermal and static disorder in absorber-scatterer distances); ΔE_0 is edge-energy shift (the difference between the zero kinetic energy value of the sample and that of the theoretical model). R factor is used to value the goodness of the fitting.

Error bounds that characterize the structural parameters obtained by EXAFS spectroscopy were estimated as N ± 20%; R ± 1%; σ^2 ± 20%; ΔE_0 ± 20%.

Table S2. Comparison of HER performance between Pt-SAs/C and other electrocatalysts in acidic media.

Catalyst	Loading mass density (mg cm^{-2})	Current density (mA cm^{-2})	Overpotential at j (mV)	Tafel slop (mV dec^{-1})	References
Pt-SAs/C	0.5	10	38	43	This work
20% Pt/C	0.5	10	36	31	This work
Pt1/MC	0.385	10	23	26	*Nat. Commun.* **2017**, 8, 1490.
Pt-MoS_2	0.075	10	53	40	*Nat. Commun.* **2013**, 4, 1444.
Pt-GDY2	$4.65*10^{-3}$ (Pt)	10	30	38	*Angew. Chem. Int. Ed.* **2018**, 57, 1
Pt_1/graphene	0.51	10	~52.2	42	*Nat. Energy* **2019**, 4, 512.
Pt_1/OLC	0.51	10	38	36	*Nat. Energy* **2019**, 4, 512.
Pt SAs/DG	1.0	10	23	25	*J. Am. Chem. Soc.* **2019**, 141, 4505.
Pt@PCM	-	10	139	65	*Sci. Adv.* **2018**, 4, eaao6657.
Pt/vertical graphene	-	10	60	28.5	*J. Mater. Chem. A* **2017**, 5, 22004
ALD 50 Pt/NGNs	0.0765	10	40	29	*Nat. Commun.* **2016**, 7, 13638.
Pt_1/NPC	$3.8*10^{-3}$ (Pt)	10	25	28	*ACS Catal.* **2018**, 8, 8450
Pt nanocuboids/ rGO	0.17	10	75	29	*J. Power Sources* **2015**, 285, 393.

Table S3. The performance comparison of this work with other similar composites.

Photocatalyst	Light source	H_2 production rate	Quantum efficiency	Ref.
CdS/m-TiO_2/G	Visible-light irradiation (≥ 420nm)	9.5 mmol g^{-1} h^{-1}	9% at 420 nm	*Nano Energy.* **2018**, 47, 8.
2.5 wt.%Ti_3C_2/CdS	Visible-light irradiation (> 420 nm)	14.34 mmol h^{-1} g^{-1}	40.5% at 425 nm	*Nat. Commun.* **2017**, 8, 13907.
16 wt.% WS_2/CdS	150 W Xe lamp (≥ 420nm)	185.79 mmol h^{-1} g^{-1}	40.5% at 420 nm	*Adv. Funct. Mater.* **2017**, 27, 1604328.
5 wt.% CoP/CdS	LED light source (30 × 3 W, λ > 420 nm)	254 mmol g^{-1} h^{-1}	25.1% at 420 nm	*Chem. Commun.* **2015**, 51, 8708
CdS/Ni@C	Visible-light irradiation (> 420 nm)	76.2 mmol h^{-1} g^{-1}	31.2% at 420 nm	*Small*, **2018**, 14, 1801705.
CdS/NiOx	Visible-light irradiation (> 420 nm)	5.91 mmol h^{-1} g^{-1}	8.6% at 420 nm	*Appl. Catal. B-Environ.* **2014**, 152, 68.
CdS/Graphene	Visible-light irradiation (≥ 420nm)	56.0 mmol h^{-1} g^{-1}	22.5% at 400 nm	*J. Am. Chem. Soc*. **2017**, 133, 10878.
CdS/MoS_2-Graphene	Visible-light irradiation (> 420nm)	9.0 mmol h^{-1} g^{-1}	28.1% at 400 nm	*ACS Nano* **2014**, 8, 7078.
11 wt.% WS_2/CdS	Visible-light irradiation (> 420nm)	1.98 mmol h^{-1} g^{-1}	N/A	*Angew. Chem. Int. Ed*. **2015**, 54, 1210.
MoS_2/rGO/TiO_2	UV–Vis (Xenon lamp)	2.066 mmol h^{-1} g^{-1}	9.7% at 365 nm	*J. Am. Chem. Soc.* **2012**, 134, 6575.
3.0 wt.% CoP/g-C_3N_4	Visible-light irradiation (> 420nm)	96.2 μmol h^{-1}	12.4% at 420 nm	*Adv. Funct. Mater.* **2017**, 27, 1604328.
CdS/Ni_2P	Visible-light irradiation (> 420nm)	1.2 mmol h^{-1} g^{-1}	41% at 450 nm	*Energ Environ Sci.* **2015**, 8, 2668.
23 mol.% $Ni(OH)_2$/CdS	Visible-light irradiation (> 420nm)	5.084 mmol h^{-1} g^{-1}	28% at 420 nm	*Green Chem*. **2011**, 13, 2708.
2 wt.% Pt-SAs/C@CdS	Visible-light irradiation (> 420nm)	310 mmol h^{-1} g^{-1}	41.2% at 400 nm	**This work**